**Engineering and Technology Journal**
**Journal homepage:** https://etj.uotechnology.edu.iq

# Physical and Electrical Properties of Spray Coating Graphene Films: The Effect of Solution Concentration

**Ayat M. Yahy[a], Evan T. Salim[a]*, Azhar I. Hassan[a], Subash C.B. Gopinath[b,c,d]**

[a] Applied Science Dept., University of Technology-Iraq, Alsina'a street, 10066 Baghdad, Iraq.
[b] Institute of Nano Electronic Engineering, Universiti Malaysia Perlis (UniMAP), 01000 Kangar, Perlis, Malaysia.
[c] Faculty of Chemical Engineering & Technology, Universiti Malaysia Perlis (UniMAP), 02600 Arau, Perlis, Malaysia.
[d] Micro System Technology, Centre of Excellence (CoE), Universiti Malaysia Perlis (UniMAP), Pauh Campus, 02600 Arau, Perlis, Malaysia.
*Corresponding author Email: evan.t.salim@uotechnology.edu.iq

## HIGHLIGHTS

- High-quality graphene Nanofilm has been deposited
- Graphene film nanostructure Layer by Layer was fabricated and characterized
- Due to its applications in advanced technologies considerable focus has been attached to the synthesis of graphene films

## ARTICLE INFO

**Handling editor:** Makram A. Fakhri

**Keywords:**

Graphene films
Spray coating
Transparent conductive films
Optical properties
Structural properties

## ABSTRACT

Graphene nanofilms were deposited by the spray coating method at different concentrations (0.05, 0.1, 0.2, 0.3, 0.4, and 0.5 g) and prepared at 120°C. The prepared nanofilms were characterized in terms of their structural, morphological, optical, and electrical properties. The results confirm the formation of high-purity and high-crystallinity graphene nanofilms with a layered nanosheet morphology. The X-ray diffraction pattern shows the presence of pure graphene with (002) crystal planes. SEM Images show that the intended graphene films are symmetrical with few wrinkles on their surface. The graphene films show semi-transparent behavior with a maximum transmission of 50%. Raman spectroscopy shows that the relative intensity, position, and shape of the G and 2D Raman peaks change with the number of graphene layers. The electrical conductivity increases with temperature, and the conductivity can be further increased depending on the metal or metal oxide functionalization. The electrical conductivity of the graphene film deposited at a concentration of 0.3 g was significantly higher than the values reported for other concentrations. The results of this study suggest that the physical and electrical properties of spray-coated graphene films can be optimized by controlling the solution concentration, which could have potential applications in transparent conductive films.

## 1. Introduction

Graphene has attracted much attention due to its exceptional properties, including conductivity, porosity, elasticity, and large surface area [1]. As the newest member of the nanocarbon family, graphene is a two-dimensional, $sp^2$-bonded carbon material that exhibits a honeycomb crystal lattice structure with a carbon-carbon bond spacing of about 0.142 nm in a single graphene sheet [2,3]. Its unique properties have made it a popular choice for various applications such as transparent conducting electrodes and large capacitors . Graphene also exhibits strong mechanical properties, crucial electrical conductivity [4], high barrier properties, and good catalytic properties [5-7]. However, the structure and properties of graphene may vary depending on the production method used. Graphene films have been produced by various methods, such as chemical vapor deposition [8], spin coating, spray coating, inkjet printing, vacuum filtration, and micromechanical cleavage of graphite [9]. Each of these methods has its advantages and disadvantages and produces graphene layers of varying thickness and homogeneity. The number of layers and the dispersion efficiency of graphene layers have a significant impact on their physicochemical properties. One problem encountered in dried graphene dispersion solutions is the tendency of graphene sheets to aggregate due to van der Waals and p-p stacking interactions [10, 11]. However, when a graphene sheet interacts with uniformly distributed nanoparticles (NPs) on a surface, it can lead to a highly defined new graphene with a specific surface area. In addition, NPs can act as stabilizers and prevent the formation of individual graphene sheets that bind together via strong van der Waals interactions. Many studies have investigated the interaction of metal oxides with graphene nanoparticles such as $TiO_2$, $SnO_2$, and $Fe_2O_3$ [12]. The main negative



http://doi.org/10.30684/etj.2023.139463.1430
Received 02 April 2023; Accepted 14 May 2023; Available online 14 June 2023
2412-0758/University of Technology-Iraq, Baghdad, Iraq

aspects of graphene are as follows (i) its fabrication is not scalable, (ii) it has no functional groups (which are required for adsorption of gasses/vapors), and (iii) it has no band gap [13-15].

The properties of graphene are influenced by factors such as the number and thickness of graphene layers and the density of defects [16,17]. Due to its ultrathin thickness and unique nanostructure, graphene can act as an impermeable film for small gas molecules [18]. Several studies have been conducted to fabricate graphene films with highly transparent conductive properties, such as the 2013 work by Xiying Ma and Hao Zhang, which investigated the CVD process, and the 2014 study by Fatima Tuz Johra et al. which investigated the assembly of graphene on a solution-based platform. In 2016, Arshad Wazir et al. fabricated graphene nanosheets by rapidly reducing microwave-induced electrically exfoliated graphene oxide. However, a common problem in fabricating transparent conductive electrodes with graphene nanomaterials is agglomeration of the nanomaterial on the surface.

Recently, graphene-based materials have attracted much attention in various fields, including energy storage systems, electronics, chemical sensors, optoelectronics, nanocomposites, and even in healthcare, e.g., as osteogenic materials [19]. To overcome the challenges in depositing graphene films, researchers have explored alternative methods such as spray deposition. Deposition of thin films from solutions by spray deposition has gained interest due to several advantages over conventional methods. These include the ability to deposit films with large surface area, low-cost preparation, cost efficiency, equipment without vacuum, and flexibility [20].

Compared to spin coating, spray coating does not require adding organic additives to the solution to increase adhesion or prepare the substrate surface to improve adhesion. This technique is easy to use, adaptable, and affordable, and it does not require any chemicals or substrate preparation. Researchers have studied the structural, electrical, and optical properties of spray-coated graphene sheets at different concentrations. In particular, a concentration of 0.3 g yielded significantly higher values compared to recently reported results at other concentrations. The properties of spray-coated graphene sheets can be used for various purposes, including transparent conductive films.

## 2. Materials

Slides of the soda-lime glass of about (2×1.5 cm) were used as substrates for the deposition of graphene films. It is important to clean the substrates as impurities will affect them. To remove impurities and dust before deposition, the glass substrate was washed with alcohol and placed in an ultrasonic bath for 20 (minutes). Then the substrate was washed with distilled water and dried with dry nitrogen gas. To prepare the graphene film, 20 (mL) spray solutions were used at concentrations of 0.05, 0.1, 0.2, 0.3, 0.4, and 0.5 (g). The solutions were sprayed onto the substrate, which was heated to a temperature of 120 (℃). The flow rate of the solution was (5 mL/min), and the carrier gas was compressed air. The distance between the substrate and the nozzle was 30 (cm). Dimethylformamide (DMF), one of the most commonly used solvents to prepare graphene, was used to scatter these graphene samples. DMF with a purity of 99.9% was purchased from Sigma-Aldrich (Sigma-Aldrich Company Ltd., Gillingham, UK) for use in this study. Use a magnetic stirrer for 60 (minutes) to prepare homogeneous solutions.

After spraying, the substrates were kept on a heater and cooled to room temperature. An X-ray diffractometer (XRD6000, Shimadzu, Japan) with Cu Kα-line radiation (λ = 1.5406Å) was used to analyze the crystalline structures and phases. The morphology of the deposited films was characterized with an atomic force microscope AFM (Ntegra NT-MDT). The spectral transmission was measured with a UV-Visible/NIR spectrophotometer (JASCO V780). Scanning electron microscope (SEM), (TESCAN, Vega III, Czech Republic) was used for Raman spectroscopy (Senterra Raman Microscope, Bruker, Germany).

## 3. Results and Discussion

Figure 1(a-f) represents the XRD patterns of graphene films produced at a deposition temperature of 120°C with different concentrations of graphene . The diffraction peak at 2θ approximately 26.5° is seen in the figure which is due to the stacking of graphene layers at the substrate surface with different graphene concentrations 0.05, 0.1, 0.2, 0.3, 0.4, 0.5 (g). The crystal plane showed the typical (002) diffraction peaks indicating the formation of graphene through spray pyrolysis. The intensity of the (002) peak tells us something about the thickness of the nanosheets. The diffraction spectrum shows that the intensity of the preferred direction increases with increasing graphene concentration. The XRD result of graphene is in good agreement with the previously published reports on graphene [20].

SEM was used to examine the surface morphology of the films as they were being deposited (SEM). Typical SEM pictures of a graphene sheet are shown in Figure 2. The SEM images show that the intended graphene films are symmetrical with few wrinkles on their surface. Characteristic wrinkled transparent regions are observed. The flaky appearance and tortuous intrinsic nanosheets of graphene are both inherent properties of the material [21].

The three main bands of interest (G-band, D-band, and 2D-band) in the Raman spectra of graphene are shown in Figure 2. The bands represent the number of graphene layers and the sample quality. D and 2D bands are always present, with the D band observed only in samples with defects. The G-band, which is localized around 1580 ($cm^{-1}$), is the most essential spectral property of graphene. It is extremely sensitive to stress effects and is related to the number of graphene layers. The status of the G-band shifts to lower frequencies as the number of layers increases. Also, the G-band is susceptible to doping. The D band, also known as the perturbation band, is created by a shift in the lattice away from the center of the Brillouin zone and has a frequency dependency on the laser. The Raman spectra of a graphene structure can be seen in Figure 3, which normally includes three primary bands: D at 1352 ($cm^{-1}$), G at 1584 ($cm^{-1}$), and 2D at 2660 ($cm^{-1}$). When the Raman shift is 1352 ($cm^{-1}$), there is a prominent D peak caused by a structural fault inside the graphene's carbon lattice. The D band, also known as the disorder band or the defect band, illustrates a ring breathing mode from sp2 C rings, however, it is only active when it is close to a graphene

edge or a defect.With high-quality graphene, the D band is often weak as well. If the D band is significant,it indicates that the graphene has many defects. The intensity of the D band is related to the amount of flaws in graphene.When the Raman shift is 1584 ($cm^{-1}$),the in-plane vibration of an sp2 hybrid carbon atom produces the other G peak.When the Raman shift is 2660 ($cm^{-1}$),the stacking mode between C atoms induces a 2D peak, however,the intensity of the 2D peak is not significant. As a result, even when no D band is present, the 2D band is always strong in graphene and does not reflect imperfections. Apart from the three unique peaks stated above, the spectrum also features an order Raman scattering peak with a Raman shift of 2910 ($cm^{-1}$). As a result, graphene nanosheets have a multi-layered structure [22-25].

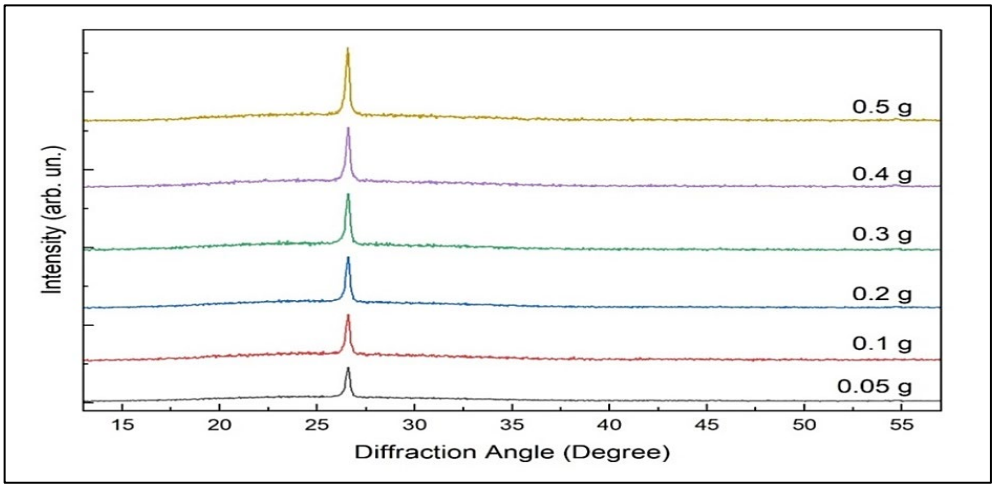


**Figure 1:** XRD of the graphene film deposited on glass at 120 (℃)

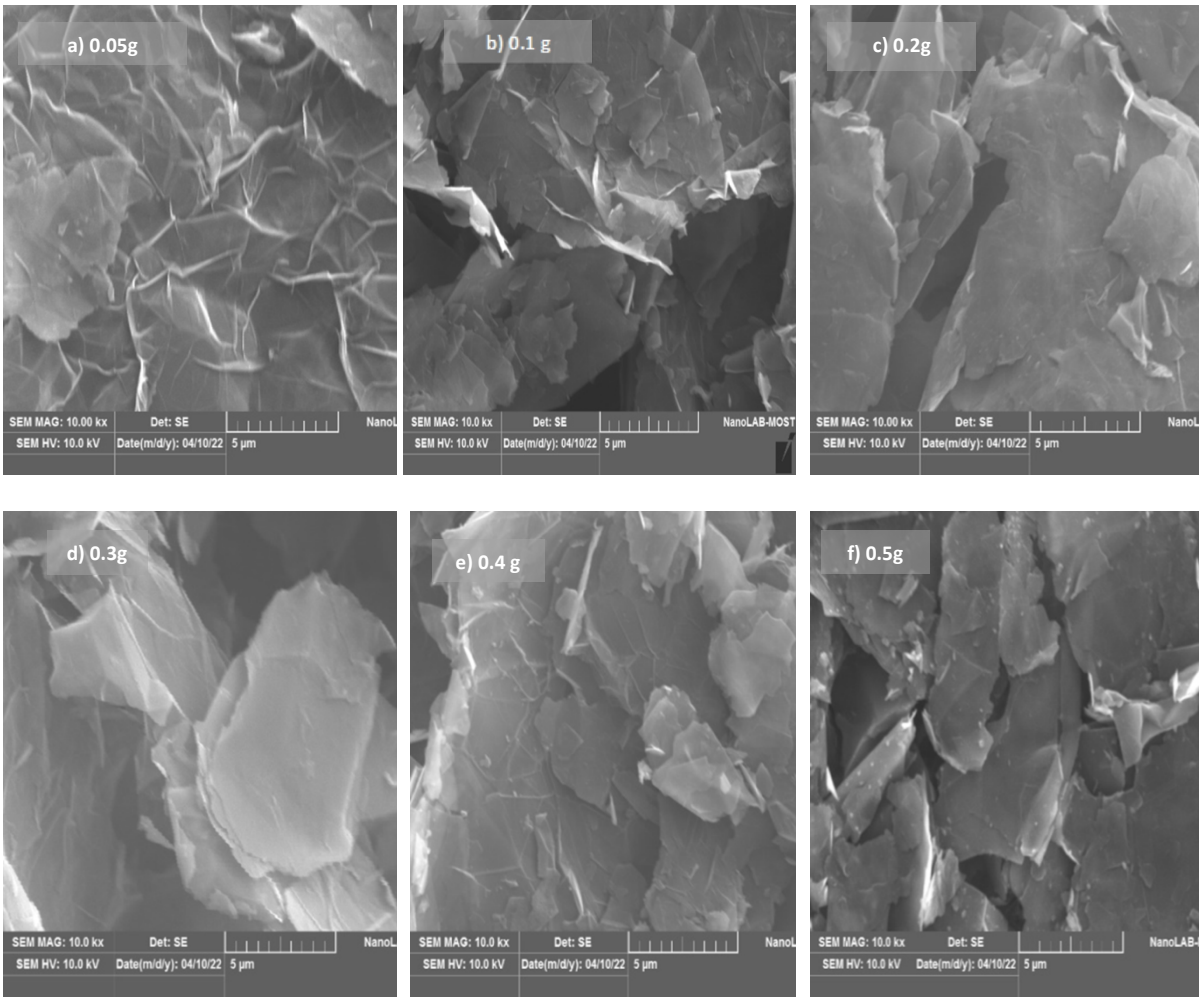


**Figure 2:** SEM Image of the graphene film deposited on glass at 120 (℃) with different concentrations

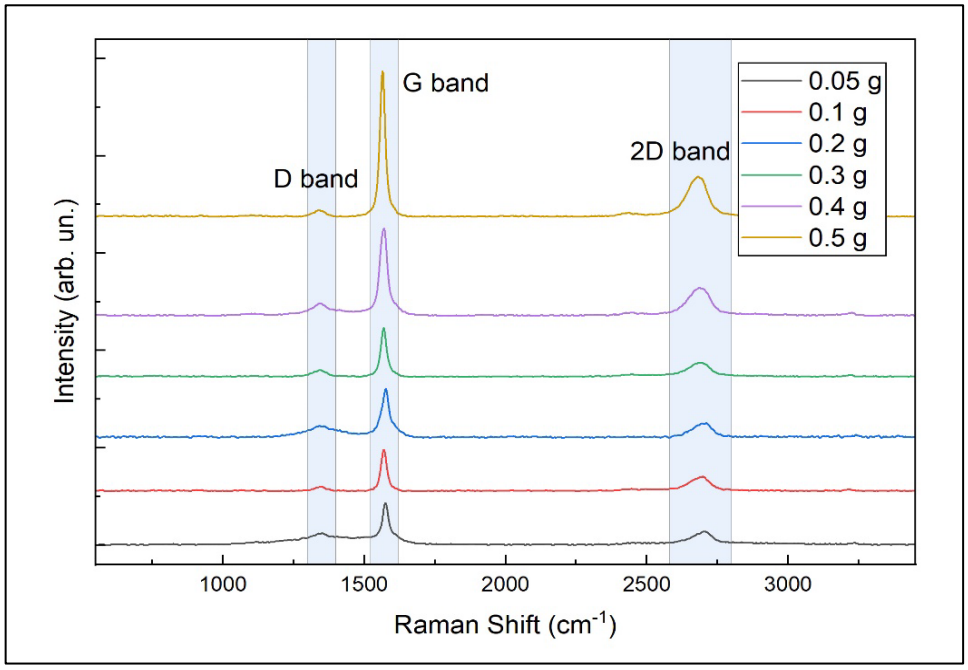


**Figure 3:** Raman Spectroscopy analysis for graphene films at different concentrations (0.05, 0.1, 0.2, 0.3, 0.4, 0.5) g

The visible light transmission rate of graphene samples is shown in Figure 4. When graphene concentration is increased. The optical transparency decreases with increasing film thickness. In contrast, the transparency of the low-focus sample increases by 50% in the visible wavelength range of 400-800 (nm) and increases with wavelength. At long wavelength light range 600-800 (nm), the films of graphene were transparent. The higher transmittance is extremely beneficial for optoelectronic devices because the light in (400-800 nm) range has high energy. The transmittance of graphene samples (in the 1000-3000 nm) wavelength near-infrared region. The transmittance was constant in the infrared wavelength range, except 2750-3000 (nm), when it increased by approximately 2.5%. The lowest transmittance of the samples in the visible and near-infrared region was more than 50%, which is consistent with the optical case of the transparent conductive films. The transparency of graphene reduced dramatically as its thickness increased. The exceptional transparency of our samples can be due to the graphene films' many graphene flakes, which allow light to pass through small holes between the flakes [26].

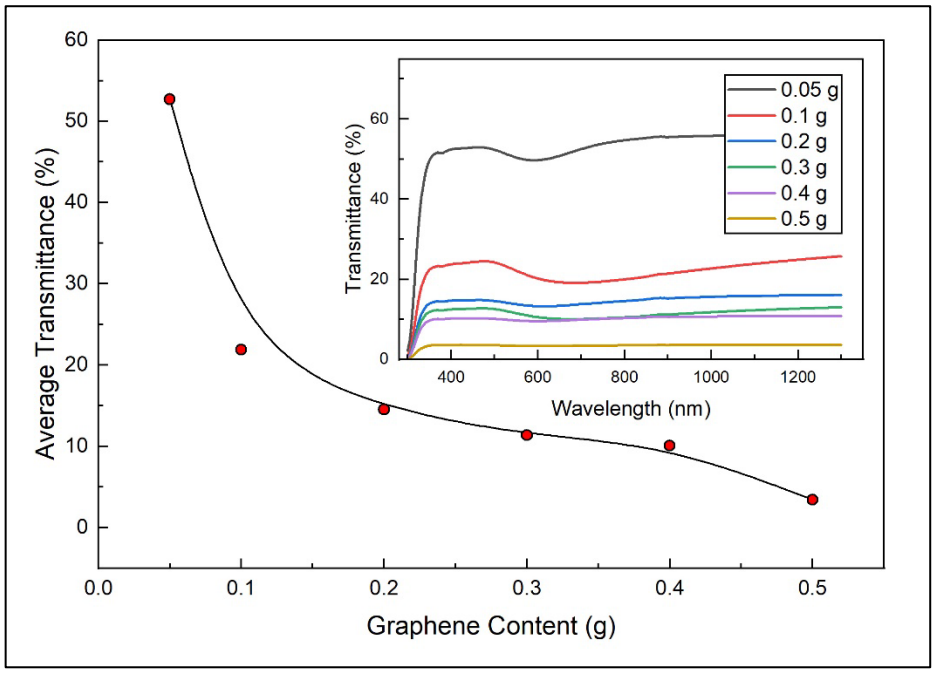


**Figure 4:** Average transmission with graphene content and light transmission of graphene sample range from (400 -1300 nm)

The electrical resistance of the prepared films was measured by heating the films at 30-150°C and determining the change in resistance of the films at different temperatures. One of the characteristics of semiconductors is the continuous increase in

conductivity values with increasing temperature. Figure 5 displays the change in (lnσ) as a function of temperature for graphene film. The electrical conductivity increases with increasing temperature, and the conductivity of graphene can be increased depending on metal or metal oxide functionalization. Graphene conducts electricity because it has free electrons moving along its structure. The two-dimensional hexagonal structure of carbon allows for the free packing of electrons in the graphene material. The electric flux travels easily through graphene, making it a superconductor of electricity. Graphene conducts electricity due to the drift of electrons that can carry electric current and pass electric flow through the material.

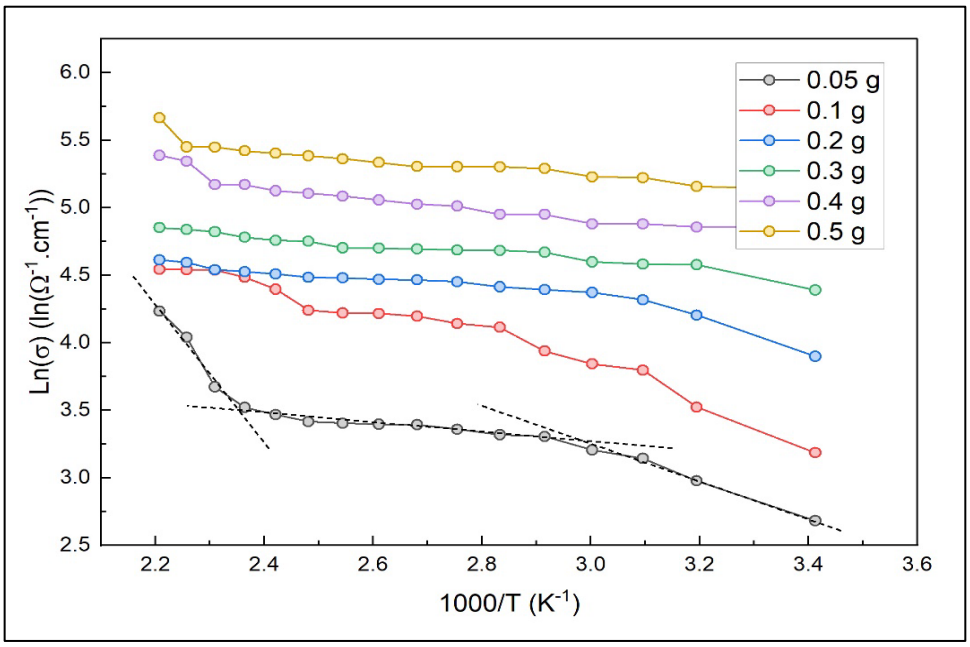


**Figure 5:** The variation of (lnσ) as a function of the reciprocal of temperature for graphene films

Figure 6 of merit (FOM), which is an optimization between electrical conductivity and optical transparency, can be determined from an estimated FOM, and the performance of the transparent conductive film can be evaluated using the following Equation 1:

$$F.O.M = 1/p1nT \quad (1)$$

where ρ is sheet resistance (Ω.cm) and T is the average of transmittance, Derived from FOM in this study, (0.3) was much higher than recently reported values at other graphene concentrations.

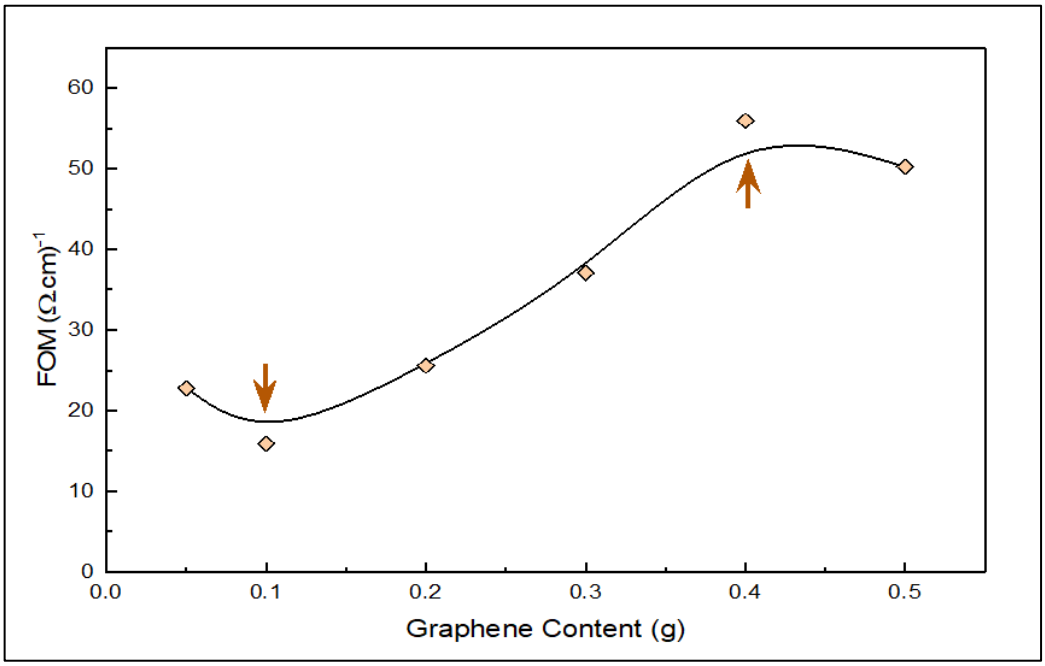


**Figure 6:** The figure of merit with graphene concentration

## 4. Conclusion

In this study, graphene films at different concentrations (0.05, 0.1, 0.2, 0.3, 0.4, and 0.5 g) were deposited on glass substrates using the spray coating method at a temperature of 120°C. The structural properties confirmed the formation of a layered nanosheet morphology, and high-purity and high-crystallinity nanofilms were produced. X-ray diffraction showed the typical (002) diffraction peak, indicating the formation of graphene by spray pyrolysis. SEM Images showed that the graphene films were symmetrical with few wrinkles on their surface. Raman spectroscopy showed that the relative intensity, position, and shape of the G and 2D Raman peaks changed with the number of graphene layers. The optical properties of the graphene films allowed the formation of semi-transparent films with a maximum transmittance of 50%. The electrical conductivity of the films increased with increasing temperature, and the conductivity of graphene can be increased depending on metal or metal oxide functionalization. The FOM value of the graphene film deposited at a concentration of 0.3 g was much higher than recently reported values at other concentrations. The results show that the physical and electrical properties of the spray-coated graphene films can be optimized by controlling the solution concentration. The high transparency and conductivity of the films suggest potential applications in transparent conductive films. These findings may be valuable for further research and development of graphene-based materials for various optoelectronic applications.

### Author contribution

Conceptualization, Evan, Azhar, and Subash; methodology, Ayat, Evan, and Azhar; software, Ayat, Evan, and Azhar; validation, Ayat, Evan, Azhar, and Subash; formal analysis, Ayat, Evan, Azhar, and Subash; investigation, Ayat, Evan, Azhar, and Subash; resources, Suhair, Ayat, Evan, and Azhar; data curation, Ayat, Evan, and Azhar; writing—original draft preparation, yat; writing—review and editing, Evan, and Subash; visualization, Evan, Azhar, and Subash; supervision, Evan, and Azhar; project administration, Evan, and Azhar; funding acquisition, Ayat, Evan, and Azhar, All authors have read and agreed to the final version of the manuscript.

### Funding

This research received no specific grant from any funding agency in the public, commercial, or not-for-profit sectors.

### Data availability statement

The data that support the findings of this study are available on request from the corresponding author.

### Conflicts of interest

The authors declare that there is no conflict of interest.

## References

**[1]** A. AlShammari, M. M. Halim, F. K. Yam, N. H. Al-Hardan, N. H. M. Kaus, K. Umar, and M. N. M Ibrahim, The effect of substrate temperatures on the structural and conversion of thin films of reduced graphene oxide, Phys. B Condens. Matter, 572 (2019) 296-301. https://doi.org/10.1016/j.physb.2019.07.018

**[2]** L. M. Malard, M. A. Pimenta, G. Dresselhaus, and M. S. Dresselhaus, Raman spectroscopy in graphene, Phys. Rep., 473 (2009) 51-87. https://doi.org/10.1016/j.physrep.2009.02.003

**[3]** W. W. Liu, S. P. Chai, A. R. Mohamed, and U. Hashim, Synthesis and characterization of graphene and carbon nanotubes: A review on the past and recent developments, J. Ind. Eng. Chem., 20 (2014) 1171-1185. https://doi.org/10.1016/j.jiec.2013.08.028

**[4]** R. R. Nair, P. Blake, A. N. Grigorenko, K. S. Novoselov, T. J. Booth, T. Stauber, and A. K. Geim, ,Fine structure constant defines visual transparency of graphene, Science, 320 (2008) 1308-1308. https://doi.org/10.1126/science.1156965

**[5]** B. Seger, P. V. Kamat, Electrocatalytically active graphene-platinum nanocomposites. Role of 2-D carbon support in PEM fuel cells, J. Phys. Chem. C, 113 (2009) 7990-7995. https://doi.org/10.1021/jp900360k

**[6]** W. Cai, Y. Zhu, X. Li, R. D. Piner, and R. S. Ruoff, Large area few-layer graphene/graphite films as transparent thin conducting electrodes, Appl. Phys. Lett., 95 (2009) 123115. https://doi.org/10.1063/1.3220807

**[7]** X. Li, Y. Zhu, W. Cai, M. Borysiak, B. Han, D. Chen, and R. S. Ruoff, Transfer of large-area graphene films for high-performance transparent conductive electrodes, Nano Lett., 9 (2009) 4359-4363. https://doi.org/10.1021/nl902623y

**[8]** G. Nandamuri, S. Roumimov, and R.Solanki, Chemical vapor deposition of graphene films, Nanotechnology, 21 (2010) 145604. https://dx.doi.org/10.1088/0957-4484/21/14/145604

**[9]** R. R. Nair, P. Blake, J. R. Blake, R. Zan, S. Anissimova, U. Bangert, T. Latychevskaia, Graphene as a transparent conductive support for studying biological molecules by transmission electron microscopy, Appl. Phys. Lett., 97 (2010) 153102. https://doi.org/10.1063/1.3492845

**[10]** L. M. Viculis, J. J. Mack, O. M. Mayer, H. T. Hahn, and R. B. Kaner, Intercalation and exfoliation routes to graphite nanoplatelets, J. Mater. Chem., 15 (2005) 974-978. https://doi.org/10.1039/B413029D

**[11]** C. Nethravathi, E. A. Anumol, M. Rajamathi, and N. Ravishankar, Highly dispersed ultrafine Pt and PtRu nanoparticles on graphene: formation mechanism and electrocatalytic activity, Nanoscale, 3 (2011) 569-571. https://doi.org/10.1039/C0NR00664E

**[12]** J. Liu, S. Fu, B. Yuan, Y. Li, and Z. Deng, Toward a universal adhesive nanosheet" for the assembly of multiple nanoparticles based on a protein-induced reduction/decoration of graphene oxide, J. Am. Chem. Soc., 132 (2010) 7279-7281. https://doi.org/10.1021/ja100938r

**[13]** N. J. Bell, Y. H. Ng, A. Du, H. Coster, S. C. Smith, and R. Amal, Understanding the enhancement in photoelectrochemical properties of photocatalytically prepared TiO2-reduced graphene oxide composite, J. Phys. Chem. C, 115 (2011) 6004-6009. https://doi.org/10.1021/jp1113575

**[14]** G. Lu, K. Yu, L. E. Ocola, and J. Chen, Ultrafast room temperature NH3 sensing with positively gated reduced graphene oxide field-effect transistors, Chem. Commun., 47 (2011) 7761-7763. https://doi.org/10.1039/C1CC12658J

**[15]** X. Huang, N. Hu, R. Gao, Y. Yu, Y.Wang, Reduced graphene oxide–polyaniline hybrid: preparation, characterization and its applications for ammonia gas sensing, J. Mater. Chem., 22 (2012) 22488-22495. https://doi.org/10.1039/C2JM34340A

**[16]** P. A. Russo, N. Donato, S. G. Leonardi, S. Baek, D. E. Conte, G. Neri, and N. Pinna, Room-temperature hydrogen sensing with heteronanostructures based on reduced graphene oxide and tin oxide, Angew. Chem. Int. Ed., 51 (2012) 11053-11057. https://doi.org/10.1002/anie.201204373

**[17]** F. Miao, S. Wijeratne, Y. Zhang, U. C. Coskun, W. Bao, and C. N Lau, Phase-coherent transport in graphene quantum billiards, science, 317 (2007) 1530-1533. https://doi.org/10.1126/science.1144359

**[18]** S. Adam, E. H. Hwang, E. Rossi, and S. D. Sarma, Theory of charged impurity scattering in two-dimensional graphene, Solid State Commun., 149 (2009) 1072-1079. https://doi.org/10.1016/j.ssc.2009.02.041

**[19]** R. M. Obodo, I. Ahmad, and F. I. Ezema, Introductory chapter: graphene and its applications, In: Graphene and Its Derivatives-Synthesis and Applications. Intechopen, 2019. https://doi.org/10.5772/intechopen.86023

**[20]** J. S. Bunch, S. S. Verbridge, J. S. Alden, A. M. Van Der Zande, J. M. Parpia, H. G. Craighead, and P. L. McEuen, Impermeable atomic membranes from graphene sheets, Nano Lett., 8 (2008) 2458-2462. https://doi.org/10.1021/nl801457b

**[21]** X. Wang, and L. Zhang, Green and facile production of high-quality graphene from graphite by the combination of hydroxyl radical and electrical exfoliation, RSC Adv., 8 (2018) 40621-40631. https://doi.org/10.1039/C8RA07880G

**[22]** M. S. Poorali, and M. M. Bagheri-Mohagheghi, Effect of the graphene doping level on the electrical and optical properties of indium tin oxide (ITO) films prepared by spray pyrolysis, J. Mater. Sci. Mater. Electron., 27 (2016) 10411-10420. https://doi.org/10.1007/s10854-016-5128-7

**[23]** L. M. Malard, M. A. Pimenta, G. Dresselhaus, and M. S Dresselhaus, Raman spectroscopy in graphene, Phys. Rep., 473 (2009) 51-87. https://doi.org/10.1016/j.physrep.2009.02.003

**[24]** A. C. Ferrari, J. C. Meyer, V. Scardaci, C. Casiraghi, M. Lazzeri, F. Mauri, and A. K. Geim, Raman spectrum of graphene and graphene layers, Phys. Rev. Lett., 97 (2006) 187401. https://doi.org/10.1103/PhysRevLett.97.187401

**[25]** F. Rashiddy Wong, A. Ahmed Ali, K. Yasui, and A. M. Hashim, Seed/catalyst-free growth of gallium-based compound materials on graphene on insulator by electrochemical deposition at room temperature, Nanoscale Res. Lett., 10 (2015) 1-10. https://doi.org/10.1186/s11671-015-0943-y

**[26]** X. Ma, and H. Zhang, Fabrication of graphene films with high transparent conducting characteristics, Nanoscale Res. Lett., 8 (2013) 1-6. https://doi.org/10.1186/1556-276X-8-440